Redefined Strategies to generate Conditional miR-141/200c miRNA cluster Knockout mice to eliminate confounding neo cassettes

Rashmi Srivastava[1#], Sanjeev Kumar Yadav[1#], Mary-Catherine Cormier[1], Kathie Lowther[2], Siu-Pok Yee[2], and Rajkumar Verma[1*]

[1]Department of Neurosciences, UConn Health Farmington CT 06030

[2]Center for Mouse Genome Modification, UConn Health, Farmington CT 06030

[#]equal contribution

*Corresponding author

Abstract:

MicroRNAs (miRNAs) of the miR-200 family specifically miR-141 and miR-200c regulate neurogenesis, differentiation, and epithelial–mesenchymal transitions in development and several diseases including cancer and stroke. The STOCK Mirc13^{tm1Mtm} /Mmjax mouse line, which targets the miR-141/200c cluster, was originally described by Park et al. (2012) as a conditional "knockout-first" allele requiring a two-step breeding strategy: Flp recombination to excise lacZ/neo cassettes followed by Cre recombination to delete the floxed miRNA cluster. However, subsequent studies frequently bypassed this step and reported knockouts based on direct crosses with Cre mouse lines, leaving residual lacZ/neo sequences that may silence upstream elements or introduce transcriptional artifacts. Here, we present a detailed and refined strategy to generate both global and tissue-specific miR-141/200c knockouts that adheres to the original design intent and eliminates confounding cassettes. Our approach confirmed robust baseline expression of miR-141 and miR-200c in various organs such olfactory bulbs and lungs where these miRNAs are robustly expressed, with near-complete loss of expression in knockout animals as validated by qPCR and in situ hybridization. By restoring a clean floxed allele prior to Cre deletion, we establish a reliable and interpretable mouse model for dissecting the roles of the miR-141/200c cluster miRNA in various disease models in these mice.

Introduction

microRNAs (miRNAs) are small, noncoding, endogenous RNAs ~22 nucleotides long. They were first described in species *C. elegans* [1,2] and were largely thought to be unique to the roundworm. However, it was not until 7 years later that they were discovered to be widely conserved across multiple species, including humans [3]. Since then, miRNAs have been extensively studied, have been implicated in a multitude of diseases [4, 5, 6], and have proven themselves to be a promising foundation for novel therapeutics [4,7].

Many of these miRNA studies have utilized cell cultures and patient tissues, limiting findings to *in vitro* settings. There was a need for *in vivo* models to better characterize miRNAs in both physiological and pathological conditions. To meet these needs, one

study employed high-throughput recombineering protocols exclusively on mouse:human conserved miRNAs to generate conditional reporter-tagged knockout-first mouse lines [8]. One such generated line targeted the cluster miR141-200c, a pair of two miRNAs from the miR-200 family that are located close together on mouse chromosome 6. These cluster miRNAs have been implicated in neurogenesis [9, 10], embryonic stem cell differentiation [11], epithelial to mesenchymal transformation [12, 14], tumorigenesis [13, 14], metastasis [13, 14, 15], stroke [16, 24], Alzheimer's Disease [17], wound healing [18], and other diseases [19, 20], making this mouse model a valuable tool in a wide variety of studies.

During the generation of this line, a targeting vector was electroporated into embryonic stem (ES) cells[8]. While this targeting vector mimicked the region of the genome that produced the miR141-200c cluster, it also introduced a lacZ tag, a β-actin-neo cassette, FRT sites, and loxP sites (Figure 1). Two breeding strategies were proposed by the contributing authors: one wherein the conditional reporter-tagged knockout-first mutant crossed with a FLP-expressing mouse, and another wherein the knockout-first mutant crossed directly with a Cre-expressing mouse[8].

While undoubtedly a sturdy foundation upon which to start, this line leaves a few loose ends which must first be addressed prior to experimental use. One such problem, as identified also by the contributing authors but did not resolve, is the silencing of the adjacent upstream genetic element[8]. Another issue that may arise from breeding strategies is the unintentional generation of chimeric mice. While the proposed FLP cross would generate an untagged conditional miRNA knockout without silencing the upstream genetic element, the Cre cross would generate a tagged but potentially chimeric mouse comprising a mix of up to four genotypes—depending on Cre efficiency—while effectively knocking out the upstream genetic element (Fig.1a). While maintaining the lacZ tag in the Cre cross is a valuable tool in expression profiling, further use may be limited due to the aforementioned silencing and chimerism[8,23].

Therefore, we explored two different strategies for generating knockouts, evaluating how each approach impacts the expression of miR-141/200c aiming to establish the most efficient and practical approach .We focused on the FLP breeding scheme to clear ambiguity about use of this mouse line given that fact that subsequent studies who used these mice did not follow up the authors plan to generate this miR-141/200c cluster KO mice either due to incomplete information or absence of clear strategy. Here, we present detailed strategies and characterization for the generation of both a global and tissue-specific miR141-200c knockout line with minimal genetic confounding factors and wide applicability. The goal of this manuscript is to present a simple and straightforward approach to generate global and cell specific KO of miR141/200c family cluster. We also review the genetic concepts that shaped our approach.

Methods

Experimental Mice

All mouse strains used in this study were obtained from the Jackson Laboratory (Farmington, CT). The STOCK Mirc13^{tm1Mtm}/Mmjax line (RRID: MMRRC_034657-JAX) is heterozygous for the targeted allele, which includes a lacZ reporter, a β-actin-neo cassette, and a floxed miR-141/200c cluster locus (lacZ-neo-flox). These mice are commonly referred to as miR-141/200c knockout (KO) mice and will be described as such throughout this study.

The B6.129S4-Gt(ROSA)26Sor^{tFLP})Sor/J (ROSA-FLPo) strain (RRID:IMSR_JAX:012930) is homozygous for the FLPo deleter allele, which carries an SA-Flpo-PGK-neo-pA cassette. Additional Cre-driver lines obtained from Jackson Laboratory included Hprt-Cre (129S1/Sv-Hprt1^{tm1(CAG-cre)Mnn}/J) (RRID: IMSR_JAX:004302)and LysM-Cre (B6.129P2-Lyz2^{tm1(cre)Ifo}/J) (RRID: IMSR_JAX:004781). Female Hprt-Cre mice, heterozygous for the targeted allele, express Cre recombinase under the PGK promoter, enabling efficient deletion of loxP-flanked genes as early as the zygote or early cleavage stages.

All mice were maintained under standard conditions at ambient temperature and humidity, with ad libitum access to pellet food and water.

Genomic DNA isolation

Mice tails (4mm) were snipped and collected in DNase free 1.5ml microcentrifuge tubes. These tail snips were incubated in 40µl digestion buffer (25mM NaOH and 0.2mM EDTA) and 1µl Proteinase K at 56ºC for overnight. The samples were then heated at 100 °C for one hour and further the reaction is neutralized by 40µl of neutralization buffer (40mM Tris buffer, pH 7.5). This crude DNA is precipitated using equal amount of ice-cold isopropanol. The precipitated DNA is suspended in 30µl of DNase free water.

PCR amplification and agarose gels electrophoresis

All mice were genotyped by PCR amplification of the relevant transgenes within the targeted alleles using their respective primer pairs (Table 1). With the exception of the forward primer for the miR-KO allele, all primers were obtained from The Jackson Laboratory's official database to ensure accuracy and reproducibility. The forward primer for the miR-KO allele (P10) was specifically designed in this study to amplify the region confirming deletion of the miR-141/200c cluster (Fig. 1a, Table 1). Conventional PCR was carried out using 2x JumpStart™ Taq ReadyMix (Sigma-Aldrich, P2893) with 50 ng of genomic DNA, 0.2 µM of each primer, and nuclease-free water to adjust the final reaction volume. PCR cycling conditions consisted of six steps: an initial denaturation at 94 °C for 3 minutes, followed by 35 cycles of denaturation (94 °C for 30 seconds), annealing (temperature and duration dependent on the targeted allele), and extension (72 °C for 30–45 seconds). This was followed by a final extension at 72 °C for 4 minutes, and a hold at 4 °C for 10 minutes. PCR products were resolved on 2% agarose gels. Agarose gels

were prepared using low EEO agarose (Fisher BioReagents, BP160-500) dissolved in 1X Tris-Acetate-EDTA (TAE) buffer (50X TAE, Bio-Rad, 1610743) by boiling. SYBR™ Safe DNA Gel Stain (Invitrogen, S33102) was added to the molten agarose as recommended by the manufacturer prior to casting in UV-transparent trays. Electrophoresis was performed in 1X TAE buffer at 50 V for 40 minutes, and bands were visualized using a gel documentation system.

Global Knockout Line Maintenance

Heterozygous KO/+ mice were crossed to each other. This cross would generate KO/KO homozygotes that would be used in experiments to assess the miR141-200c knockout phenotype, KO/+ heterozygotes which would be used to refresh the maintenance line, and WT mice which would be used as age- and litter-matched controls to the KO/KO experimental homozygotes.

Tissue-Specific Knockout Line Maintenance

Fl/fl, LysMCre/+ mice were crossed with fl/fl, WT mice. All the progeny from this cross would be fl/fl homozygotes. Half would be hemizygous for the LysMCre and half would be WT for the LysMCre. To avoid knocking out the Lyz2 gene, LysMCre/LysMCre homozygotes should always be avoided. Mice with fl/fl, LysMCre/+ genotypes would be considered experimental mice, while mice with fl/fl, WT genotypes would be considered age- and litter-matched controls.

β-Galactosidase (lacZ) Staining

A β-galactosidase reporter gene staining kit (Sigma-Aldrich, GALS, St. Louis, MO, USA) was used for lacZ reporter analysis. Mice designated for lacZ staining were deeply anesthetized with a single intraperitoneal injection of Avertin (250 mg/kg body weight) and perfused intracardially with 40 mL of ice-cold 1× PBS and brains were then extracted. In a cryostat, 10 μm brain sections were cut and mounted on Superfrost Plus charged slides, and staining was performed according to the manufacturer’s protocol. Briefly, sections were washed with 1× PBS and fixed with the provided fixation solution for 10 minutes at room temperature. The staining solution was prepared in 1× PBS by mixing reagents A, B, C, and X-Gal solution (40 mg/mL). After washing, the staining solution was applied to the sections, followed by incubation at 37°C for 0.5–2 hours. After incubation, the staining solution was removed, and the sections were mounted using 70% glycerol and imaged.

RNA isolation, cDNA synthesis and real-time PCR

Total RNA (including small RNA) was isolated from the tissues of the different brain regions, including olfactory bulbs, frontal cortex, parietal cortex, hippocampus and cerebellum and peripheral organs such as heart, lung, and liver using TRIzol or miRVana miRNA isolation kit (Ambion Life Technology), respectively, per manufacturer protocol. The cDNA was synthesized for miRNA using TaqMan MicroRNA Reverse Transcription Kit (cat. no. 4366596, Thermo Fisher Scientific) according to the manufacturer's protocol.

TaqMan single-tube assay primers for miR-141-3p (no. 000463), miR-200c-3p (002300), and U6 snRNA (no. 001973) were procured from Thermo Fisher Scientific. TaqMan universal PCR master mix II, no UNG (cat. no. 4440040) was procured from Thermo Fisher Scientific. Relative quantification of gene expression was performed using the comparative Ct method ($2^{-\Delta\Delta Ct}$) with U6 snRNA as normalization control.

RNA-fluorescence in situ hybridization (FISH)

RNA-FISH was performed according to the manufacturer's instructions (Molecular Instruments). In brief, tissue sections were post-fixed with 4% paraformaldehyde (PFA) for 15 minutes and washed with 1× PBS. Sections were then pre-hybridized with probe hybridization buffer in a humidified chamber at 37 °C for 10 minutes. After incubation, the hybridization buffer was replaced with 1.6 pmol of probe solution (miR-141-3p), and the sections were incubated overnight (>12 hours) at 37 °C in the humidified chamber. The following day, excess probes were removed by sequential washes with a decreasing gradient of 5× SSCT. Amplification buffer was then added to the sections, and pre-amplification was carried out in a humidified chamber at room temperature (RT) for 30 minutes. In parallel, 6 pmol each of hairpin h1 and h2 were prepared by snap cooling (heated at 95 °C for 90 seconds, then cooled to RT in the dark for 30 minutes). The hairpin solution was prepared by adding the snap-cooled h1 and h2 hairpins to 100 µl of amplification buffer at RT. Following pre-amplification, the buffer was removed from the sections and replaced with the prepared hairpin solution. The samples were then incubated overnight (>12 hours) at RT in a humidified chamber. After a final series of washes with 5× SSCT, the samples were mounted using antifade DAPI UltraCruz Mounting Solution (Santa Cruz Biotechnology, Cat. No. SC-24941) and imaged.

Gene targeted	Direction and Name	Primer Sequence (5'-3')	Amplic on size
Targeted miR cluster-generating site	Forward Primer (P5)	CAA CAG CCT CTG ACC TTT AAC C	432bp
	Reverse Primer (P6)	CCT TCT GGG CAG ACA AGA ATA C	
miR cluster-generating site (WT)	Forward Primer (P5)	CAA CAG CCT CTG ACC TTT AAC C	340bp
	Reverse Primer (P6)	CCT TCT GGG CAG ACA AGA ATA C	
lacZ	Forward Primer (P1)	ATC CTC TGC ATG GTC AGG TC	315 bp
	Reverse Primer (P2)	CGT GGC CTG ATT CAT TCC	
	Forward Primer (P3)	CTT GGG TGG AGA GGC TAT TC	280bp

β-actin-neo cassette	Reverse Primer (P4)	AGG TGA GAT GAC AGG AGA TC	
mir KO (mir5'Fn3')	Forward Primer (P10)	CCG GCA GGT GAA GGA GGA AG'	~300 bp
	Reverse Primer (P6)	CCT TCT GGG CAG ACA AGA ATA C	
FLPo	Forward Primer (P7)	AAA GTC GCT CTG AGT TGT TAT	300 bp
	Reverse Primer (P8)	GCG AAG AGT TTG TCC TCA ACC	
	Forward Primer (P7)	AAA GTC GCT CTG AGT TGT TAT	603 bp
	Reverse Primer (P9)	GGA GCG GGA GAA ATG GAT ATG	
HprtCre (Cre recombinase)	Forward Primer (P11)	GCG GTC TGG CAG TAA AAA CTA TC	100 bp
	Reverse Primer (P12)	GTC AAA CAG CAT TGC TGT CAC TT	
LysMCre (Cre recombinase)	Forward Primer (P13)	CTT GGG CTG CCA GAA TTT CTC	700bp
	Reverse Primer (P14)	CCC AGA AAT GCC AGA TTA CG	
	Forward Primer (P13)	CTT GGG CTG CCA GAA TTT CTC	350 bp
	Reverse Primer (P15)	TTA CAG TCG GCC AGG CTG AC	

Table1. List of different sets of primer sequences (with amplicon size) used in PCR amplification

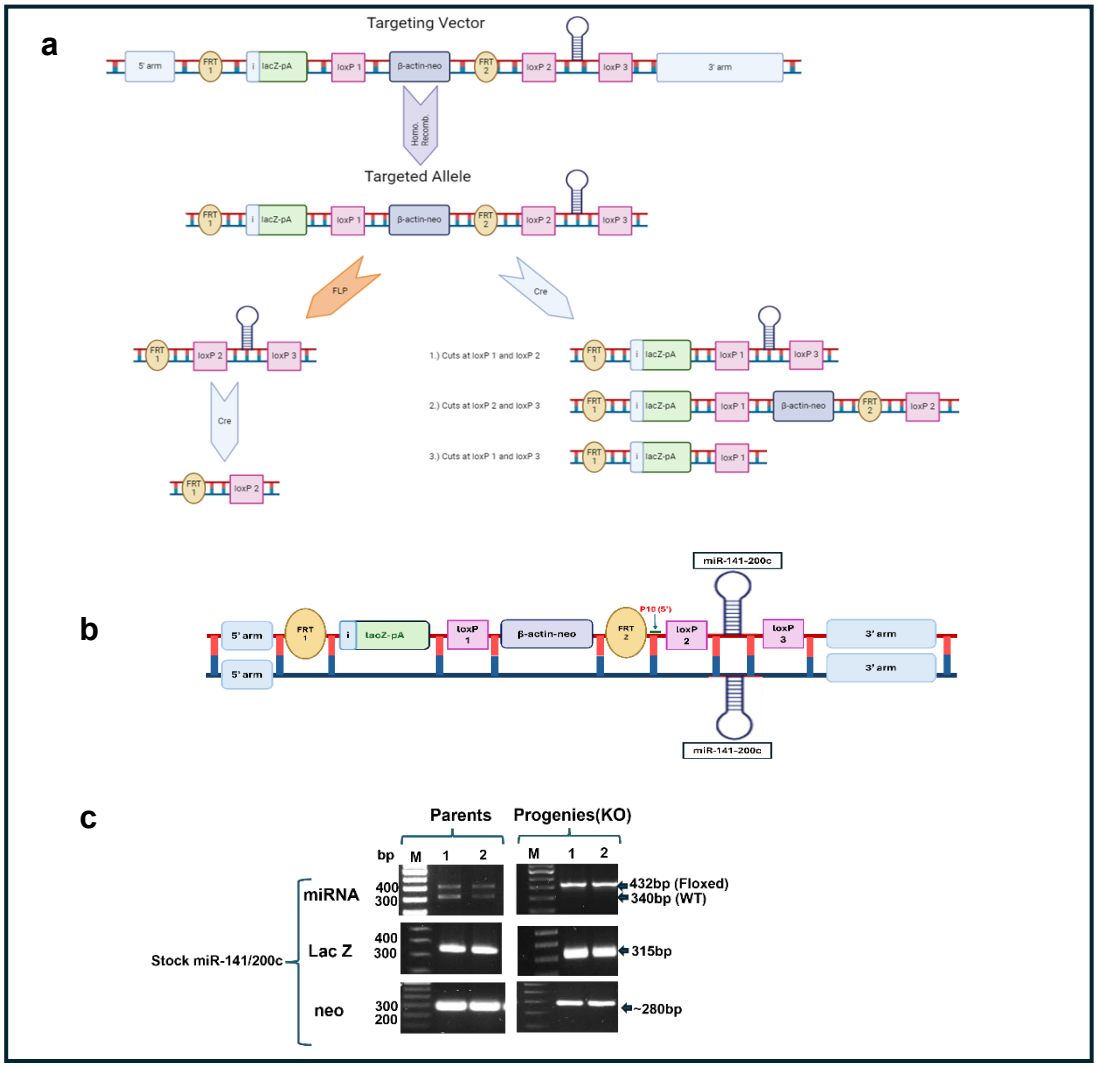

Figure 1: a) Schematic representation of the gene targeting strategy and allele modification process for conditional knockout generation. The top panel ("Targeting Vector") illustrates the original targeting construct containing 5' and 3' homologous arms, a lacZ reporter with polyadenylation signal (lacZ-pA), loxP and FRT sites, and a β-actin-neo selection cassette. The middle panel ("Targeted Allele") shows the correctly integrated targeted allele after homologous recombination, with all key elements positioned between loxP and FRT sites. The lower panels illustrate recombinase-mediated excision outcomes: FLP recombinase excises the β-actin-neo cassette at FRT sites, and Cre recombinase mediates excision at different combinations of loxP sites (loxP1/loxP2, loxP2/loxP3, or loxP1/loxP3), yielding multiple possible allelic configurations. These steps enable precise control over gene disruption and regulatory element removal, facilitating conditional knockout and downstream genetic analyses. **b)** Representation of Primer position binding on the targeted allele: Forward primer (P10) was designed to screen homozygous miR-141/200c-knockout (miR-KO) so that it binds to the upstream of loxP-2 site which is also upstream of mir-141/200c allele. **c)** PCR validation of miR-141-200c alleles and the generation of homozygous knockout of miR-141/200c: Agarose gels showing PCR-genotyping results of targeted alleles in parents (first set) and screening of progenies on 2% agarose gels (second set) where miRNA (miR-141/200c), lacZ, neo are showing the PCR results of their expression. Lane M is the DNA ladder lane, lanes-1 and 2 are mouse #1 and mouse#2. PCR analysis of genomic DNA from various mouse lines shows expected band sizes corresponding to wild-type (WT) and mutant (Mut) alleles for both miR-141-200c

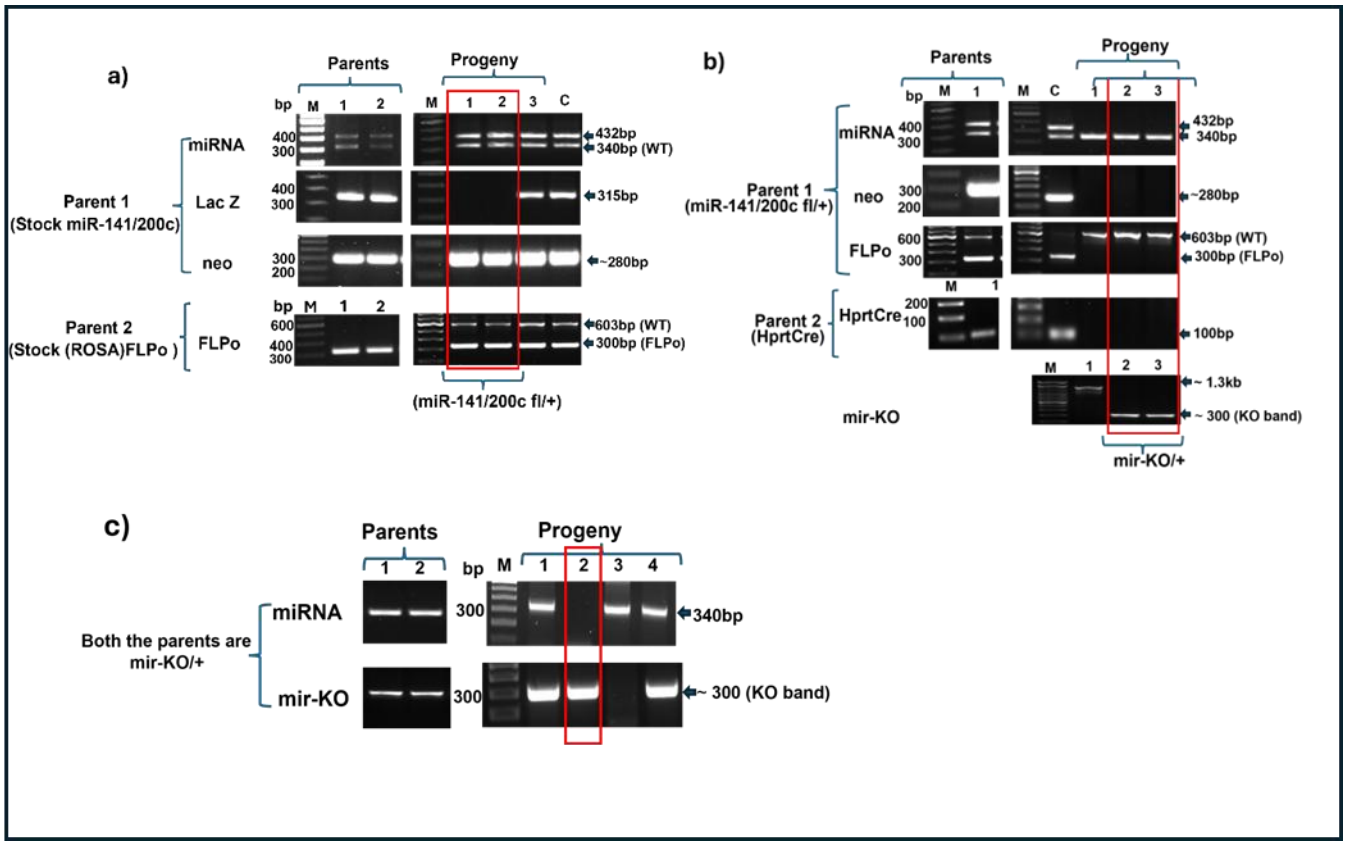

Figure. 2. Genotype screening of transgenic mice. Agarose gels showing PCR results of targeted alleles in parents (first set) and progeny screening on 2% gels (second set). **a**) Generation of heterozygous conditional knockouts mediated by FLP alleles. Offspring yielding a 603 bp FLPo amplicon, 432bp (floxed miR-141/200c) and loss of the *lacZ* allele were selected for further breeding with Cre deleter mice. **b**) Generation heterozygous miR-141/200c knockout (mir-KO/+) mediated by Cre. Offspring from the crossing of floxed miR-141/200c with HprtCre mice were PCR-genotyped for the targeted allele (miRNA), neo, FLPo and HprtCre. The homozygous miR-141/200c knockout mice were selected which showed WT for miR-141/200c (340bp), FLPo (603bp), neo (no band) and HprtCre (no band) genotype, and loss of floxed-mir-141/200c allele (~300bp). **c**) Generation of litter- and aged-offsprings from crossing mir-KO/+ male mice with HprtCre female mice. PCR-genotyping of offsprings for the miR-141/200c showed either WT band

Results

Breeding Strategies for the Generation of Knockout Mice

Two breeding strategies have been used to achieve mir-141/200c-knockout mice.

Strategy 1: Generation of homozygous Stock miR-141/200c - global Knockout Mice (S_1GKO):

Stock miR-141/200c X Stock miR-141/200c

As mentioned earlier, the stock miR-141/200c KO mice were generated as conditional lacZ reporter-tagged knockout-first mouse strains for miR-141/200c[8]. The high-efficiency polyadenylation signal terminates transcription, thereby preventing expression of downstream exons i.e. expression of miR-141/200c [8, 21, 22]. Prior to generating the mouse

model, the stock miR-141/200c mice were PCR-genotyped to validate the targeted alleles (lacZ-neo-flox) (Fig.1c. After the validation, these stock miR-141/200c mice were inter-crossed to generate homozygous S_1GKO (Fig.1c). We screened the offsprings by PCR-genotyping for targeted allele of the stock miR-141/200c mice that includes a lacZ tag, a β-actin-neo cassette (neo), and the miR-cluster-generating site (miRNA). Amplicons confirming wild-type (WT) and homozygous-knockout of the miR-14-locus yielded single bands, 340bp and 432bp, respectively, and the heterozygous strain yielded double bands-340bp and 420bp. The amplicon of lacZ tag and β-actin-neo cassette alleles yielded single bands as 315bp and 280bp, respectively, in both hetero- and homozygous offsprings, (Fig.1c). Together, these results confirmed the successful insertion of the lacZ–neo–flox alleles mediated by homologous recombination, thereby establishing a knockout-first mouse line. We selected these homozygous knockouts (S_1GKO) and their littermate WT for further validation of this mouse line.

Strategy 2: Generation of mir-141/200c-global Knockout Mice (S_2GKO):

Generation of Flp-mediated heterozygous conditional knockout (CKO): Stock miR-141/200c X Stock (ROSA)FLPo

For the generation of S2GKO, firstly, we crossed the stock miR-141/200c mice with homozygous (ROSA)FLPo mice. The offspring from this cross were PCR-genotyped to check for deletion of the lacZ tag. PCR amplicons corresponding to the lacZ–neo–flox alleles and the FLPo deleter allele were analyzed by agarose gel electrophoresis. The results showed that the lacZ allele was excised in pups #1 and #2, whereas in pups #3 and #4, PCR products yielded a 315 bp band, confirming the presence of the lacZ allele and inheritance of the lacZ–neo–flox allele (Fig. 1a, 2a). Although excision of the lacZ tag and β-actin–neo cassette was expected by Flp recombinase, in some cases the Flp-mediated excision was not fully penetrant. Consequently, residual lacZ or β-actin–neo sequences were occasionally detected in the progeny, reflecting incomplete recombination efficiency at the FRT sites[8]. It was expected that both the lacZ tag and β-actin–neo cassette would be excised from progeny inheriting the targeted allele from the miR-141/200c parent; indeed, loss of the lacZ tag indicated concurrent loss of the β-actin–neo cassette, since both elements are located between the two FRT sites. However, because the (ROSA)FLPo targeted allele carries a PGK–neo cassette and the stock (ROSA)FLPo breeder is homozygous for this allele, all progeny from this cross were heterozygous for the (ROSA)FLPo transgene. PCR genotyping confirmed this, yielding amplicons corresponding to the wild-type (300 bp) and the FLPo deleter allele (603 bp). As a result, the β-actin–neo cassette from the miR-141/200c targeted allele was absent, whereas the PGK–neo cassette from the (ROSA)FLPo targeted allele was retained and detected by the generic neo PCR assay (280 bp) (Fig.2a). In the progeny that inherited the miR-141/200c targeted allele, the Flp recombinase enzyme would always be present to excise the lacZ tag and β-actin-neo cassette and modify the miR-targeted allele in the progeny that inherited it by cleaving at the two FRT sites [8] (Figure 1). This would excise the lacZ tag, a loxP site, and the β-actin-neo cassette, leaving behind a residual FRT site

and an miR cluster-generating site flanked by loxP sites. This strategy results in the generation of a heterozygous floxed (fl) conditional knockout (CKO) allele. *Generation of FLP- mediated global knockout:*

miR141-200c fl/+, FLPo/+ X HprtCre/+

Heterozygous HprtCre/+ females were used as Cre drivers crossed with males carrying a heterozygous floxed miR-141/200c conditional knockout (CKO) allele. . The progeny that inherited floxed CKO allele and the global Cre would exhibit a knockout (KO) allele; the Cre recombinase would modify the floxed CKO allele by cleaving at the two remaining loxP sites, excising the miR cluster-generating site while leaving behind a residual loxP site (Fig.1a). After PCR-genotyping of the pups, we found that the amplicon from the pup#1 for miR cluster-generating allele (miRNA), generic neo (neo) FLPo and homozygous knockout of yielded bands at 340bp (WT), no band, 603bp and around 1.3 kb, respectively, indicating WT genotype of the pup. It should be noted that a generic neo band would be found if either the FLPo or the HprtCre gene was inherited. After generating the floxed CKO allele, the FLPo is no longer necessary and should therefore be bred out. It is for this reason that female progeny heterozygous for the miR knockout allele, heterozygous for the HprtCre (there may be condition where HprtCre may bred out in the first cross and will get heterozygous pups for the miR knockout allele), and WT for the FLPo were selected for further line development. Pups #2 and #3 showed heterozygous miR-141/200c-knockout (mir-KO/+) genotype with the virtue of this, the PCR products for miR cluster generating site and mir-KO yielded 340 bp and around 300bp, respectively, confirming the successful excision of floxed miR generating allele from one of the loci. As a virtue of this, the pups which have the genotype as pup#2 and #3 are heterozygous miR-KO. The amplicon of HprtCre allele for pup#2 and #3 did not show any band of 100bp confirming its presence. Fortunately, we found pups like we showed here as pup#2 and #3 where amplicon of HprtCre yielded no band but amplicon of mir-KO yielded band around 300bp, showing the excision of floxed-miR at a very early embryonic stage (1- or 2-cell stage). In HprtCre mice, the HprtCre gene is on an X-linked locus and is active in the female germline before egg formation. As a result, eachoocyte of these HprtCre mice expresses Cre recombinase by virtue of single allele and when such oocytes fertilized by sperm carrying a floxed allele, the Cre recombinase would trigger the recombination at a very early embryonic stage (1- or 2-cell stage), leaving heterozygous taregeted-knockout allele with no allele for Hprt CreAs during this breeding stage, we identified mice that were heterozygous for the miR knockout (miR-KO/+) in which the *Hprt-Cre* transgene had already been bred out (Fig. 2b). Therefore, these mice were not crossed further with WT animals for removal of the *Hprt-Cre* allele (Fig. 3). From this cross, these heterozygous miR-KO (miR-KO/+) offsprings (in which HprtCre and FLPo were also bred out) were used for the generation of litter-mate homozygous knockout and WT offsprings.

Global Knockout Line Maintenance: miR141-200c KO/+, X miR141-200c KO/+,

Heterozygous KO/+ mice were intercrossed with each other. This cross generated KO/KO homozygotes, which were used in experiments to assess the miR141-200c knockout phenotype; KO/+ heterozygotes, which were used to maintain the breeding line; and WT mice, which served as age- and litter-matched controls for the KO/KO experimental homozygotes. The offspring from this cross were PCR-genotyped for miR cluster-generating allele and miR-KO. Pup#1 showed homozygous mir-141/200c knockout genotype as evident by the electrophoresis result. There was no yield in the amplicon of miR-141/200c allele, but the amplicon of miR-KO PCR yielded around 300 bp (Fig. 2c). But the pup#2 and pup#3 showed WT and heterozygous knockout (**S_1GKO**) genotype (Fig.2c).

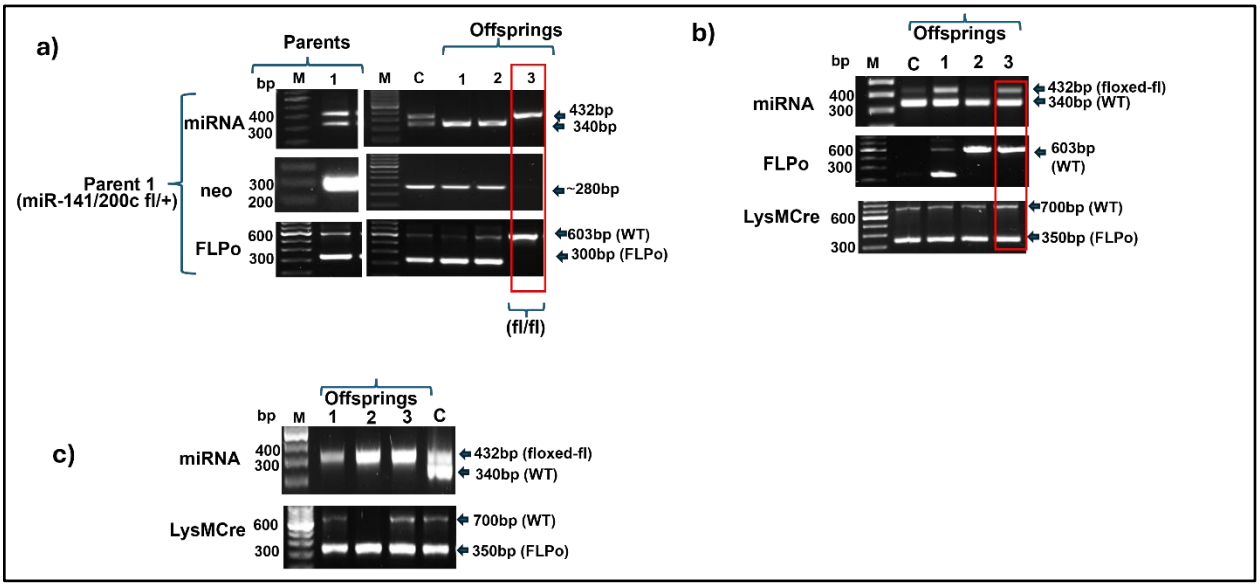

Fig.3. Generation of myeloid cell-specific homologous knockout of miR-141/200c. Multiple PCR panels indicate confirmation of floxed miR clusters, generic neo, FLPo, and LysMCre in various breeding strategies. Reproducible gel bands evidence the presence of all intended elements in offspring after the crosses. Agarose gel electrophoresis: a) presents PCR genotyping for miR141-200c fl/+, FLPo/+ × miR141-200c fl/+, FLPo/+ progeny, verifying the presence of floxed miR cluster, generic neo, and FLPo alleles, b) depicts results of miR141-200c fl/+, FLPo/+ × LysMCre/+ crosses, confirming the successful integration of the LysMCre transgene and one of the floxed alleles in the selected mice. c) confirms the integration of LysMCre and presence of floxed alleles on both the loci. Banding patterns and schematics detail the genotype structure in each experimental line. . Lane M is the DNA ladder lane, lane C is the positive controls of the respective PCR, lanes-1, 2 and 3 are respective mouse #1, #2 and #3.

Generation of myeloid cell-specific homologous knockout of miR-141/200c

miR141-200c fl/+, FLPo/+ X miR141-200c fl/+, FLPo/+

As previously discussed, the miR141-200c X (ROSA)FLPo cross would generate a floxed CKO allele. We generated floxed CKO homozygotes of miR-141/200c by inter-crossing the floxed CKO heterozygotes. Once homozygous floxed (CKO) mice have been established, breeding to produce tissue-specific knockouts—such as myeloid-specific deletions—becomes significantly more efficient, since every cross with a Cre-driver yields the desired flox/flox;Cre genotype[23]. Progeny that was homozygous for the miR floxed CKO allele and WT for the (ROSA)FLPo were selected (Fig.3a). In any mouse that inherited the (ROSA)FLPo, the generic neo PCR would detect the neo cassette's presence.

miR141-200c fl/+, FLPo/+ X LysMCre/+

Concurrently, we crossed miR141-200c fl/+ mice with LysMCre/+ cross. Heterozygous LysMCre/+ were used as Cre drivers and were crossed with mice that were heterozygous for the floxed miR141-200c CKO allele. The progeny that inherited both the floxed CKO allele and the tissue-specific Cre would exhibit a KO allele only in the specific tissue; every other tissue type—including germline cells—would show the floxed CKO allele along with the Cre (Fig.3b).

Similar to the HprtCre cross, FLPo is no longer required and should be bred out. In its absence, the generic neo PCR does not detect a neomycin resistance gene. Unlike HprtCre, however, the LysMCre-targeted allele lacks a neo cassette. For further line development, offsprings were selected as heterozygous both for the floxed miR CKO allele and LysMCre, and wild type for FLPo.

miR141-200c fl/fl X miR141-200c fl/+, LysMCre/+

In the cross between *miR141-200c fl/fl* and *miR141-200c fl/+, LysMCre/+* mice, both experimental and control cohorts are generated. Experimental mice consist of *fl/fl* homozygotes carrying the *LysMCre* transgene (*fl/fl, LysMCre/+*), whereas *fl/fl* homozygotes lacking Cre (*fl/fl, WT*) serve as controls (Fig.3c). Although these offspring can be used directly, this approach is inefficient and are not suitable for experiments. So, to optimize colony maintenance, both *fl/fl, LysMCre/+* and *fl/fl, WT* mice were retained as breeders for subsequent generations.

miR-141-3p and miR-200c-3p expression analysis *ex vivo*.

The expression patterns of miR-141-3p and miR-200c-3p were initially assessed using a lacZ reporter assay. In agreement with previous studies, the assay revealed robust enrichment of lacZ activity specifically in the adult mouse olfactory bulb, while no (undetectable via lacZ expression) expression was detectable in other brain regions. Beyond the central nervous system, low levels of lacZ expression were observed in the lungs, particularly near their junction with the respiratory tract, but were absent in other

peripheral tissues such as the heart and liver. To investigate the functional consequences of miR-141/200c cluster loss, global knockout (GKO) mice for miR-141/200c-cluster miRNA were generated using the following two strategies suggested by park et al. (2012). Following strategy (S_1), quantitative RT-qPCR analysis further confirmed that the olfactory bulb exhibited the highest basal expression of miR-141-3p and miR-200c-3p among all surveyed brain regions and peripheral organs in the littermate wild-type (S_1WT), which is consistent with the miRNA atlas [25]. The global knockout (S_1GKO) efficiency was validated by RT-qPCR, which demonstrated a near-complete ablation of target miRNA expression in the olfactory bulb and a substantial reduction in the lungs.

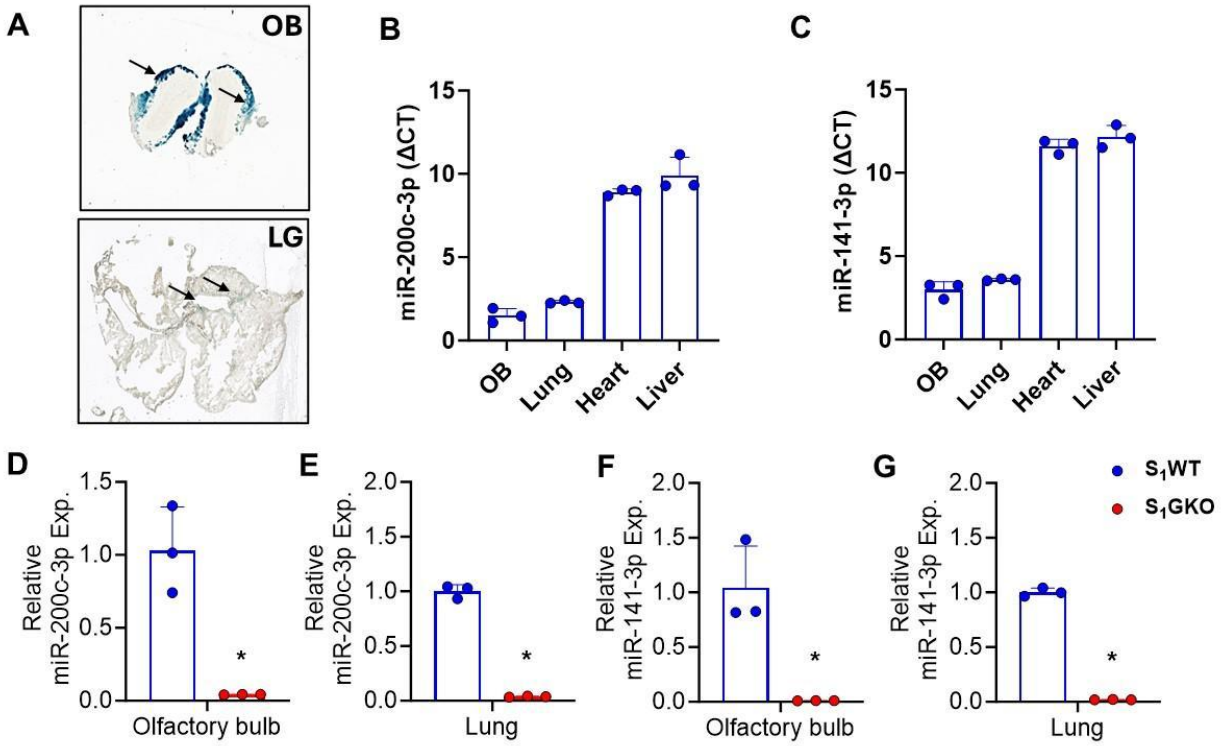

Fig 4. Expression analysis of miRNA-141/200c. miRNA-141/200c expression analyzed by lacZ reporter expression and RT-qPCR in 6–8-week-old mice. Olfactory bulb (OB) exhibited strong lacZ reporter expression for miR-141/200c whereas the lung (LG) showed localized staining near the respiratory tract attachment site (A). The basal expression of miR-141-3p and miR-200c-3p was analyzed by RT-qPCR in the brain olfactory bulb and other peripheral organs such as the lung, heart, and liver of wild-type mice. The data showed that miR-141-3p and miR-200c-3p were highly expressed in the olfactory bulb and lung ($\Delta CT < 5$), whereas heart and liver exhibited lower expression levels ($\Delta CT > 10$) (B&C). Total RNA was isolated from the brain olfactory bulb and lungs of wild-type and lacZ KO mice generated by strategy one (S_1), and relative expressions of miR-141-3p and miR-200c-3p were assessed by RT-qPCR. A significant and near-complete reduction of miR-141-3p and miR-200c-3p expression was observed in the olfactory bulb and lungs (D-G). Data are presented as mean ± SD (*$p < 0.05$ vs. WT control).

miR-141-3p and miR-200c-3p expression in littermate- S_2GKO and WT mice

The optimized strategy (S_2) produced miR-141/200c KO mice (S_2GKO) alongside appropriate controls (S_2WT). Baseline expression profiles for both miR-141-3p and miR-200c-3p were quantified across the olfactory bulb, frontal cortex, parietal cortex, hippocampus, and cerebellum of the wild-type mice (S_2WT). Consistent with initial findings, the olfactory bulb maintained the highest expression across all brain regions. Subsequent generation of global KO mice (S_2GKO) using the refined protocol with hprt cre led to significantly reduced expression of miR-141-3p and miR-200c-3p throughout the brain, with the greatest decrease observed in the olfactory bulb. These findings were corroborated by RNA *in situ* hybridization, which confirmed the complete loss of miR-141-3p in the olfactory bulb of KO mice.

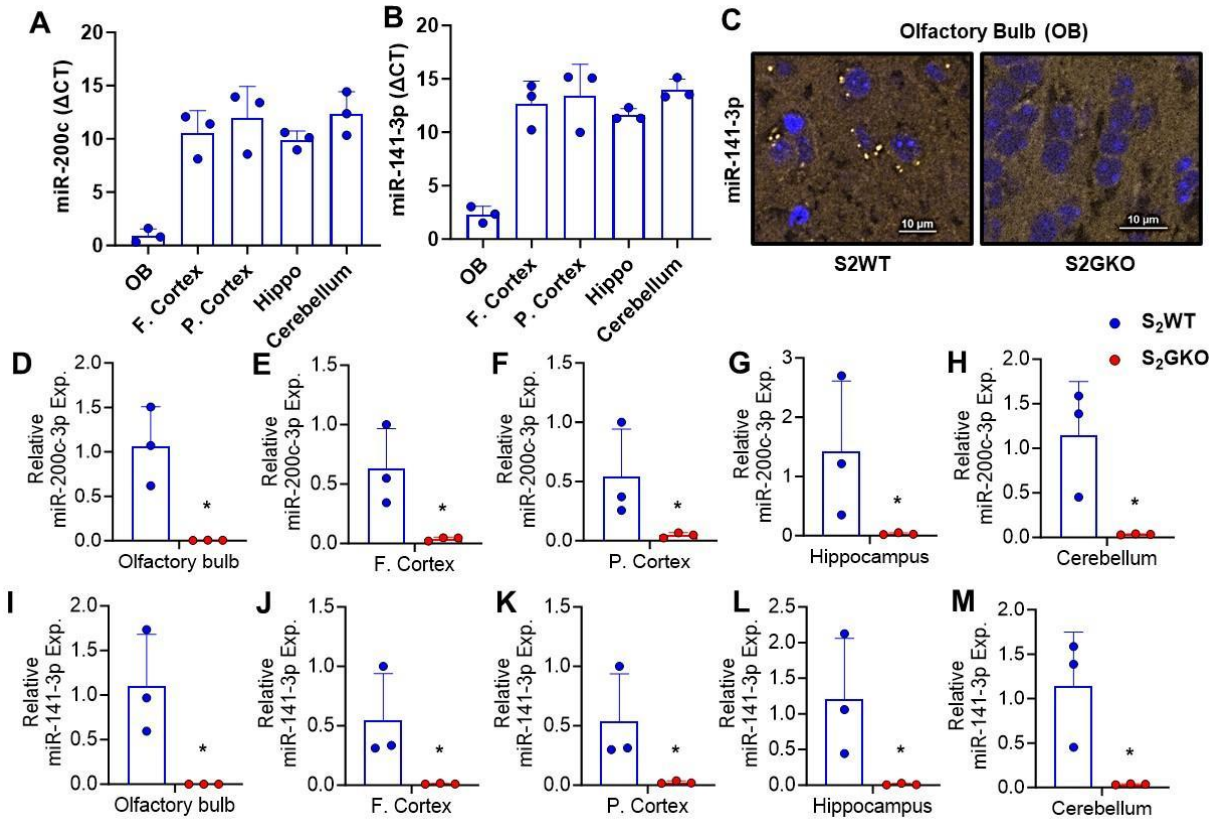

Fig.5 Expression analysis of miR-141-3p and miR-200c-3p in mice generated by strategy 2. Total RNA was isolated from the olfactory bulb (OB), frontal cortex (FC), parietal cortex (PC), hippocampus (HP), and cerebellum (CB) of wild-type (S2WT) and knockout (S2GKO) mice. Basal expression levels of miR-141-3p and miR-200c-3p were assessed by RT-qPCR in S2WT samples. Both miR-141-3p and miR-200c-3p were highly expressed in the OB ($\Delta CT < 5$), while their expression in other regions was very low ($\Delta CT > 10$) (A&B). Notably, the OB of S2GKO mice showed no detectable expression of miR-141-3p by RNA-FISH (C). This finding was further confirmed by RT-qPCR, which demonstrated a marked reduction of both miRNAs (miR-200c-3p & miR-141-3p) in the OB almost negligible (D&I), along with significantly decreased expression in the FC, PC, HP, and CB of S2GKO mice (E-H & J-M). Data are presented as mean ± SD (*$p < 0.05$ vs. WT control).

Discussion

The generation of the *mirc13tm1Mtm/Mmjax* line by Park et al. (2012) provided the first conditional knockout-first model for the miR-141/200c cluster. In their design, the targeting vector introduced a lacZ reporter and β-actin-neo cassette flanked by FRT sites, in addition to loxP sites bracketing the cluster. Park et al. explicitly recommended a two-step strategy: (1) cross with Flp deleter mice to remove the lacZ/neo cassette and restore a clean conditional (floxed) allele; and (2) use Cre recombinase to achieve either tissue-specific or global deletion of the miR-141/200c cluster. This approach avoids interference from the lacZ/neo elements, which can otherwise silence adjacent genes or alter expression patterns[26, 27]. With a splice acceptor, the lacZ tag is fused to the upstream genetic element and spatiotemporally expressed in a manner reflecting the upstream genetic element's expression[28]. While useful for expression analysis, this tag may influence the activity of the upstream genetic element to which it is bound[28]. Additionally, the poly(A) tail at the end of the lacZ tag terminates transcription, preventing the complete transcription of the element in which it is embedded and silencing any downstream elements[29]. The β-actin-neo cassette, comprising the powerful β-actin promotor and neomycin-resistance gene, is expressed regardless of the lacZ tag's presence due to said powerful promotor. Used during mouse line development to differentiate between nonhomologous and homologous recombination of the targeting vector in ES cell colonies, the β-actin-neo cassette can influence transcription of downstream genes in an unpredictable fashion[30]. It is for these reasons that both the lacZ tag and the β-actin-neo cassette must be removed prior to experimental use.

Despite this clear roadmap, several subsequent studies that employed the *mirc13tm1Mtm/Mmjax* mice appear not to have followed Park's recommended strategy. Instead, direct crosses of the lacZ-neo-flox allele to Cre deleter lines were reported as sufficient to generate knockout mice (Ref 10-14, 16-20). While this startegy produces a lacZ-tagged null allele, it also retains the β-actin-neo cassette, raising the possibility of unintended transcriptional interference and complicating phenotype interpretation as discussed above (Ref from up). In particular, incomplete reporting of breeding schemes, or reliance solely on the absence of lacZ as a surrogate for knockout status has created ambiguity in the literature regarding the true genetic state of these animals[8].

Our study addresses this gap by implementing the complete breeding strategy and detailed step wise protocol expended from original study of Park et al 2012. We also provide qPCR confirmation data in addition to lacZ staining and miRNA FISH. We first removed the lacZ/neo cassettes using (ROSA)FLPo mice, generating a clean floxed allele. Only then did we introduce Cre recombinase, either germline (Hprt-Cre) to achieve global deletion or tissue-specific (LysM-Cre) for lineage-restricted ablation. These steps ensure that any observed phenotype can be attributed directly to loss of the miR-141/200c cluster, without confounding contributions from transcriptional silencing or residual neomycin cassette effects.

This refinement is not merely technical but critical for functional interpretation. Studies of the miR-200 family—including their roles in late postnatal neurogenesis (Beclin et al., 2016), stem cell differentiation (Zhang et al., 2015), and cancer biology (Tseng et al., 2017; Chen et al., 2013; Jin et al., 2017)—rely heavily on precise gene dosage and context. Misinterpreted allele structures could mask subtle phenotypes or yield spurious results, contributing to discrepancies across reports. By clarifying the breeding approach and providing critical data support the success of our mouse model generation, our work provides a framework for generating unambiguous global and conditional knockouts of the miR-141/200c cluster.

Acknowledgment: This work was supported by NIH, United States (1R21NS114981 and R01 NS140176) and REP Convergence (OVPR UConn, United States) grant to R.V. and R.B.

Reference:

1. Rosalind C. Lee, Rhonda L. Feinbaum, Victor Ambros, The C. elegans heterochronic gene lin-4 encodes small RNAs with antisense complementarity to lin-14, Cell, Volume 75, Issue 5, 1993, Pages 843-854, ISSN 0092-8674, https://doi.org/10.1016/0092-8674(93)90529-Y
2. Bruce Wightman, Ilho Ha, Gary Ruvkun, Posttranscriptional regulation of the heterochronic gene lin-14 by lin-4 mediates temporal pattern formation in C. elegans, Cell, Volume 75, Issue 5, 1993, Pages 855-862, ISSN 0092-8674, https://doi.org/10.1016/0092-8674(93)90530-4
3. Pasquinelli, A., Reinhart, B., Slack, F. *et al.* Conservation of the sequence and temporal expression of *let-7* heterochronic regulatory RNA. *Nature* 408, 86–89 (2000). https://doi.org/10.1038/35040556
4. E. van Rooij, A.L. Purcell, A.A. Levin, Developing microRNA therapeutics, Circ. Res., 110 (2012), pp. 496-507, 10.1161/circresaha.111.247916
5. Sagar Vyavahare , Sandeep Kumar , Kathryn Smith , Bharati Mendhe , Roger Zhong , Marion A. Cooley , Babak Baban , Carlos M. Isales , Mark Hamrick , William D Hill , Sadanand Fulzele. Inhibiting MicroRNA-141-3p Improves Musculoskeletal Health in Aged Mice. *Aging and disease*. 2023, 14(6): 2303-2618 https://doi.org/10.14336/AD.2023.0310-1
6. Small, E. M., Frost, R. J., & Olson, E. N. (2010). MicroRNAs add a new dimension to cardiovascular disease. *Circulation*, *121*(8), 1022–1032. https://doi.org/10.1161/CIRCULATIONAHA.109.889048
7. Janssen, H. L., Reesink, H. W., Lawitz, E. J., Zeuzem, S., Rodriguez-Torres, M., Patel, K., van der Meer, A. J., Patick, A. K., Chen, A., Zhou, Y., Persson, R., King, B. D., Kauppinen, S., Levin, A. A., & Hodges, M. R. (2013). Treatment of HCV infection by targeting microRNA. *The New England journal of medicine*, *368*(18), 1685–1694. https://doi.org/10.1056/NEJMoa1209026
8. Park, C. Y., Jeker, L. T., Carver-Moore, K., Oh, A., Liu, H. J., Cameron, R., Richards, H., Li, Z., Adler, D., Yoshinaga, Y., Martinez, M., Nefadov, M., Abbas, A.

K., Weiss, A., Lanier, L. L., de Jong, P. J., Bluestone, J. A., Srivastava, D., & McManus, M. T. (2012). A resource for the conditional ablation of microRNAs in the mouse. *Cell reports*, *1*(4), 385–391. https://doi.org/10.1016/j.celrep.2012.02.008

9. Choi, P. S., Zakhary, L., Choi, W. Y., Caron, S., Alvarez-Saavedra, E., Miska, E. A., McManus, M., Harfe, B., Giraldez, A. J., Horvitz, H. R., Schier, A. F., & Dulac, C. (2008). Members of the miRNA-200 family regulate olfactory neurogenesis. *Neuron*, *57*(1), 41–55. https://doi.org/10.1016/j.neuron.2007.11.018
10. Beclin, C., Follert, P., Stappers, E., Barral, S., Coré, N., de Chevigny, A., Magnone, V., Lebrigand, K., Bissels, U., Huylebroeck, D., Bosio, A., Barbry, P., Seuntjens, E., & Cremer, H. (2016). miR-200 family controls late steps of postnatal forebrain neurogenesis via Zeb2 inhibition. *Scientific reports*, *6*, 35729. https://doi.org/10.1038/srep35729
11. Zhang, J., Gao, Y., Yu, M., Wu, H., Ai, Z., Wu, Y., Liu, H., Du, J., Guo, Z., & Zhang, Y. (2015). Retinoic Acid Induces Embryonic Stem Cell Differentiation by Altering Both Encoding RNA and microRNA Expression. *PloS one*, *10*(7), e0132566. https://doi.org/10.1371/journal.pone.0132566
12. Tseng, J. H., Bisogna, M., Hoang, L. N., Olvera, N., Rodriguez-Aguayo, C., Lopez-Berestein, G., Sood, A. K., Levine, D. A., & Jelinic, P. (2017). miR-200c-driven Mesenchymal-To-Epithelial Transition is a Therapeutic Target in Uterine Carcinosarcomas. *Scientific reports*, *7*(1), 3614. https://doi.org/10.1038/s41598-017-03972-7
13. Humphries, B., & Yang, C. (2015). The microRNA-200 family: small molecules with novel roles in cancer development, progression and therapy. *Oncotarget*, *6*(9), 6472–6498. https://doi.org/10.18632/oncotarget.3052
14. Chen, D., Zhang, Y., Wang, J., Chen, J., Yang, C., Cai, K., Wang, X., Shi, F., & Dou, J. (2013). MicroRNA-200c overexpression inhibits tumorigenicity and metastasis of CD117+CD44+ ovarian cancer stem cells by regulating epithelial-mesenchymal transition. *Journal of ovarian research*, *6*(1), 50. https://doi.org/10.1186/1757-2215-6-50
15. Jin, T., Suk Kim, H., Ki Choi, S., Hye Hwang, E., Woo, J., Suk Ryu, H., Kim, K., Moon, A., & Kyung Moon, W. (2017). microRNA-200c/141 upregulates SerpinB2 to promote breast cancer cell metastasis and reduce patient survival. *Oncotarget*, *8*(20), 32769–32782. https://doi.org/10.18632/oncotarget.15680
16. Verma, R., Ritzel, R. M., Harris, N. M., Lee, J., Kim, T., Pandi, G., Vemuganti, R., & McCullough, L. D. (2018). Inhibition of miR-141-3p Ameliorates the Negative Effects of Poststroke Social Isolation in Aged Mice. *Stroke*, *49*(7), 1701–1707. https://doi.org/10.1161/STROKEAHA.118.020627
17. Wu, Q., Ye, X., Xiong, Y., Zhu, H., Miao, J., Zhang, W., & Wan, J. (2016). The Protective Role of microRNA-200c in Alzheimer's Disease Pathologies Is Induced

by Beta Amyloid-Triggered Endoplasmic Reticulum Stress. *Frontiers in molecular neuroscience*, *9*, 140. https://doi.org/10.3389/fnmol.2016.00140

18. Aunin, E., Broadley, D., Ahmed, M. I., Mardaryev, A. N., & Botchkareva, N. V. (2017). Exploring a Role for Regulatory miRNAs In Wound Healing during Ageing:Involvement of miR-200c in wound repair. *Scientific reports*, *7*(1), 3257. https://doi.org/10.1038/s41598-017-03331-6
19. Ji, J., Qin, Y., Ren, J., Lu, C., Wang, R., Dai, X., Zhou, R., Huang, Z., Xu, M., Chen, M., Wu, W., Song, L., Shen, H., Hu, Z., Miao, D., Xia, Y., & Wang, X. (2015). Mitochondria-related miR-141-3p contributes to mitochondrial dysfunction in HFD-induced obesity by inhibiting PTEN. *Scientific reports*, *5*, 16262. https://doi.org/10.1038/srep16262
20. Majer, A., Caligiuri, K. A., Gale, K. K., Niu, Y., Phillipson, C. S., Booth, T. F., & Booth, S. A. (2017). Induction of Multiple miR-200/182 Members in the Brains of Mice Are Associated with Acute Herpes Simplex Virus 1 Encephalitis. *PloS one*, *12*(1), e0169081. https://doi.org/10.1371/journal.pone.0169081
21. Raja, R., Dumontier, E., Phen, A., & Cloutier, J. F. (2024). Insertion of a neomycin selection cassette in the Amigo1 locus alters gene expression in the olfactory epithelium leading to region-specific defects in olfactory receptor neuron development. *Genesis*, 62, e23594.
22. Testa G, Schaft J, van der Hoeven F, Glaser S, Anastassiadis K, Zhang Y, Hermann T, Stremmel W, Stewart AF. A reliable lacZ expression reporter cassette for multipurpose, knockout-first alleles. Genesis. 2004 Mar;38(3):151-8. doi: 10.1002/gene.20012. PMID: 15048813.
23. He B, Deckelbaum RA, Miao D, Lipman ML, Pollak M, Goltzman D, Karaplis AC. Tissue-specific targeting of the pthrp gene: the generation of mice with floxed alleles. Endocrinology. 2001 May;142(5):2070-7. doi: 10.1210/endo.142.5.8146. PMID: 11316774.
24. Yadav SK, Dhuri K, Gamiotea-Turro D, Cormier MK, Patel V, Yadawa AK, Pathuri M, Bahal R, Verma R. Exploring the therapeutic potential of sγPNA-141: Pharmacodynamics and mechanistic insights during ischemic stroke recovery. Mol Ther Nucleic Acids. 2024 Oct 9;35(4):102355. doi: 10.1016/j.omtn.2024.102355. PMID: 39507400; PMCID: PMC11539414.
25. Rishik S, Hirsch P, Grandke F, Fehlmann T, Keller A. miRNATissueAtlas 2025: an update to the uniformly processed and annotated human and mouse non-coding RNA tissue atlas. Nucleic Acids Res. 2025 Jan 6;53(D1):D129-D137. doi: 10.1093/nar/gkae1036. PMID: 39540421; PMCID: PMC11701691.
26. Branda CS, Dymecki SM. Talking about a revolution: The impact of site-specific recombinases on genetic analyses in mice. Dev Cell. 2004 Jan;6(1):7-28. doi: 10.1016/s1534-5807(03)00399-x. PMID: 14723844.
27. McBurney MW, Mai T, Yang X, Jardine K. Evidence for repeat-induced gene silencing in cultured Mammalian cells: inactivation of tandem repeats of transfected genes. Exp Cell Res. 2002 Mar 10;274(1):1-8. doi: 10.1006/excr.2001.5443. PMID: 11855851.

28. Skarnes WC, Auerbach BA, Joyner AL. A gene trap approach in mouse embryonic stem cells: the lacZ reported is activated by splicing, reflects endogenous gene expression, and is mutagenic in mice. Genes Dev. 1992 Jun;6(6):903-18. doi: 10.1101/gad.6.6.903. PMID: 1592261.
29. Nair P, Steel KP, Lewis MA. Investigating the effects of a cryptic splice site in the En2 splice acceptor sequence used in the IKMC knockout-first alleles. Mamm Genome. 2024 Dec;35(4):633-644. doi: 10.1007/s00335-024-10071-2. Epub 2024 Oct 1. PMID: 39354111; PMCID: PMC11522132.
30. Stanford WL, Caruana G, Vallis KA, Inamdar M, Hidaka M, Bautch VL, Bernstein A. Expression trapping: identification of novel genes expressed in hematopoietic and endothelial lineages by gene trapping in ES cells. Blood. 1998 Dec 15;92(12):4622-31. PMID: 9845528.